© 2014. Published by The Company of Biologists Ltd | Development (2014) 141, 1553-1561 doi:10.1242/dev.101840

RESEARCH ARTICLE

Profilin 1 is required for peripheral nervous system myelination

Laura Montani[1,2,*], Tina Buerki-Thurnherr[2,3,*], Joana Paes de Faria[1], Jorge A. Pereira[2], Nuno G. Dias[1], Rui Fernandes[1], Ana F. Gonçalves[1], Attila Braun[4], Yves Benninger[2], Ralph T. Böttcher[4], Mercedes Costell[4,5], Klaus-Armin Nave[6], Robin J. M. Franklin[7], Dies Meijer[8], Ueli Suter[2] and João B. Relvas[1,2,‡]

ABSTRACT

Myelination allows rapid saltatory propagation of action potentials along the axon and is an essential prerequisite for the normal functioning of the nervous system. During peripheral nervous system (PNS) development, myelin-forming Schwann cells (SCs) generate radial lamellipodia to sort and ensheath axons. This process requires controlled cytoskeletal remodeling, and we show that SC lamellipodia formation depends on the function of profilin 1 (Pfn1), an actin-binding protein involved in microfilament polymerization. Pfn1 is inhibited upon phosphorylation by ROCK, a downstream effector of the integrin linked kinase pathway. Thus, a dramatic reduction of radial lamellipodia formation is observed in SCs lacking integrin-linked kinase or treated with the Rho/ROCK activator lysophosphatidic acid. Knocking down Pfn1 expression by lentiviral-mediated shRNA delivery impairs SC lamellipodia formation *in vitro*, suggesting a direct role for this protein in PNS myelination. Indeed, SC-specific gene ablation of Pfn1 in mice led to profound radial sorting and myelination defects, confirming a central role for this protein in PNS development. Our data identify Pfn1 as a key effector of the integrin linked kinase/Rho/ROCK pathway. This pathway, acting in parallel with integrin β1/LCK/Rac1 and their effectors critically regulates SC lamellipodia formation, radial sorting and myelination during peripheral nervous system maturation.

KEY WORDS: Profilin, Myelination, Schwann cell, Mouse

INTRODUCTION

Schwann cells (SCs) are the myelin-forming cells of the peripheral nervous system (PNS). During development, SC precursors populate outgrowing axon bundles, where they proliferate and differentiate into immature SCs (Jessen and Mirsky, 2005). Possibly as a result of increasing cell density (Webster et al., 1973), these cells extend radial lamellae into axon bundles. SCs segregate and establish 1:1 relationships with individual large caliber (>1 μm diameter) axons. Upon maturing into the promyelinating stage, the SCs start to segregate and later myelinate such axons, leaving behind small axons that will remain unmyelinated. This process is collectively referred to as radial sorting (Webster et al., 1973), and requires the formation of a cytoplasmic protrusion radially in relation to the main SC axis, similar to a giant lamellipodia in form and function (Nodari et al., 2007; Feltri et al., 2008). Such radial lamellipodia are likely to be controlled by the same molecular machinery regulating actin polymerization at the leading edge of lamellipodia in cultured cells (Feltri et al., 2008). It is therefore important to understand which molecular players orchestrate the functional cytoskeletal remodeling that are necessary for these cellular structures to form. The small Rho GTPases Cdc42 and Rac1 are known to modulate actin cytoskeletal dynamics in SCs and regulate radial sorting. Whereas Cdc42 is mainly involved in the control of SC proliferation (Benninger et al., 2007), Rac1 promotes SC lamellipodia formation (Benninger et al., 2007; Nodari et al., 2007) downstream of laminin/integrin-β1/lymphoid cell kinase (LCK) (Feltri et al., 2002; Ness et al., 2013). Rac1 downstream targets N-WASP (Jin et al., 2011; Novak et al., 2011) and MLCK/myosin II (Wang et al., 2008; Leitman et al., 2011) are key regulators of radial sorting and PNS myelination. Negative regulation of Rho/ROCK signaling by integrin-linked kinase (Ilk) (Pereira et al., 2009) is also strictly required for SC cytoskeleton rearrangements leading to efficient radial sorting. However, the downstream mediators of Rho/ROCK have not yet been clearly identified.

Profilins (Pfns) are small, ubiquitous, 12-16 kDa actin-binding proteins. Mammals encode four different Pfn proteins, Pfn1 being the major isoform found in nearly all tissues (Witke et al., 1998). In the nervous system, Pfn1 might play a role in Huntington's disease (Shao et al., 2008), and mutations in the *PFN1* gene were recently linked to familial amyotrophic lateral sclerosis (Wu et al., 2012). Pfn2a, the only other isoform expressed in the developing nervous system (Lambrechts et al., 2000; Witke et al., 2001), has been implicated in the regulation of neuritogenesis (Da Silva et al., 2003).

Pfns are pivotal in promoting actin dynamics at the plasma membrane to drive actin-linked processes. They form 1:1 complexes with monomeric actin, regulating its availability by sequestration (Carlsson et al., 1977), and catalyze the exchange of actin-bound ADP to ATP to enable rapid microfilament polymerization (Finkel et al., 1994; Witke et al., 1998; Witke et al., 2001; Witke, 2004). Pfn1 is also a ROCK substrate. ROCK-mediated Pfn1 phosphorylation on Ser137 leads to its inactivation in both HEK293 cells and primary neurons (Shao et al., 2008). In light of the central role of Pfn in the regulation of actin dynamics and lamellipodia formation (Cao et al., 1992; Syriani et al., 2008), Pfn1 is poised as an excellent candidate to regulate myelination downstream of Rho/ROCK by potentially modulating SC radial lamellipodia formation. Using mouse genetics and *in vitro* experiments, we demonstrate a novel crucial function for Pfn1 in radial sorting and ensheathment during PNS development. Moreover, we show that Ilk/Rho/ROCK negatively controls Pfn1 function and that this signaling acts in parallel with the integrin β1/LCK/Rac1 pathway to regulate SC lamellipodia formation. Furthermore, we found that Igf1, which is produced by SCs, can inhibit Rho/ROCK signaling thereby enhancing Pfn1 function and driving radial lamellipodia formation.

[1]Instituto de Biologia Molecular e Celular, 4150-180 Porto, Portugal. [2]Institute of Molecular Health Sciences, Department of Biology, Swiss Federal Institute of Technology, ETH Zurich, 8093 Zurich, Switzerland. [3]EMPA, Swiss Federal Laboratories for Materials Testing and Research, Materials-Biology Interaction, 9014 St Gallen, Switzerland. [4]Max-Planck Institut für Biochemie, 82152 Martinsried, Germany. [5]Department of Biochemistry and Molecular Biology, Universitat de València, 46100 Burjassot, València, Spain. [6]Max-Planck Institut für Experimentelle Medizin, 37075 Göttingen, Germany. [7]Wellcome Trust-Medical Research Council, Stem Cell Institute, Cambridge CB2 2XY, UK. [8]Erasmus MC, Postbus 2040, 3000 CA Rotterdam, The Netherlands.
*These authors contributed equally to this work

‡Author for correspondence (jrelvas@ibmc.up.pt)

Received 29 July 2013; Accepted 3 February 2014

Development (2014) doi:10.1242/dev.101840

RESULTS

Rho/ROCK signaling regulates radial lamellipodia formation in SCs

Ilk-negative regulation of Rho/ROCK signaling is crucial for radial sorting and PNS myelination (Pereira et al., 2009). Such processes are thought to depend on the capacity of SCs to extend radial lamellipodia mediated by Rac1 activation downstream of integrin β1 (supplementary material Fig. S1) (Nodari et al., 2007; Feltri et al., 2008). However, *Ilk* mutant mice displayed impaired radial sorting and myelination, despite Rac1 hyperactivation (Pereira et al., 2009). We found that the numbers of radial lamellipodia in *Dhh-Cre Ilk*$^{fl/fl}$ (mutant) SCs were significantly lower compared with those in *Dhh-Cre Ilk*$^{fl/wt}$ (control) SCs (Fig. 1Aa,b). These data further support the crucial role of radial lamellipodia formation in efficient radial sorting and myelination. Furthermore, they suggest the existence of a negative signaling pathway that is able to counteract Rac1 activation of lamellipodia formation in *Ilk* mutant mice. The Rho/ROCK pathway is hyperactivated in *Ilk* mutant mice and responsible for the observed radial sorting phenotype (Pereira et al., 2009). Thus, we tested whether it could be responsible for the failure in radial lamellipodia formation. Pharmacological inhibition of ROCK by Y27632 (10 μM) or fasudil (40 μM) restored formation of radial lamellipodia in *Ilk* mutant SCs (Fig. 1Ac-f), suggesting that Rho/ROCK signaling is capable of inhibiting radial lamellipodia formation even in the presence of Rac1 hyperactivation.

Rho/ROCK regulates Pfn1 activity independently of integrin β1 and Rac1 signaling

Pfn1 is an actin remodeling protein that is capable of regulating lamellipodia formation in different cell types (Cao et al., 1992; Syriani et al., 2008), and is a ROCK substrate (Shao et al., 2008). Therefore, it is a strong candidate in mediating lamellipodia formation downstream of Rho/ROCK in SCs. To address whether Rho/ROCK signaling regulates Pfn1 in SCs, we analyzed phosphoS137-Pfn1 levels (Shao et al., 2008) in lysates obtained from rat SC cultures exposed to lysophosphatidic acid (LPA), a known SC activator of Rho signaling. Although 3 hours of LPA treatment of SCs increased phospho-Pfn1 without affecting Pfn1 total levels (Fig. 1B), exposure of LPA-treated SC to the ROCK inhibitor Y27632 (10 μM) prevented the increase in Pfn1-P levels (Fig. 1B). Very short-term exposure to LPA (<3 minutes) has been reported to transiently increase Rac1 activation in the SCL4.1/F7 SC line (Barber et al., 2004). Thus, we tested whether LPA also increased Rac1 activation in our experimental conditions, in which primary SCs were exposed to LPA for 3 hours. Although the analysis of Rac1 expression and activity by pull-down assay and

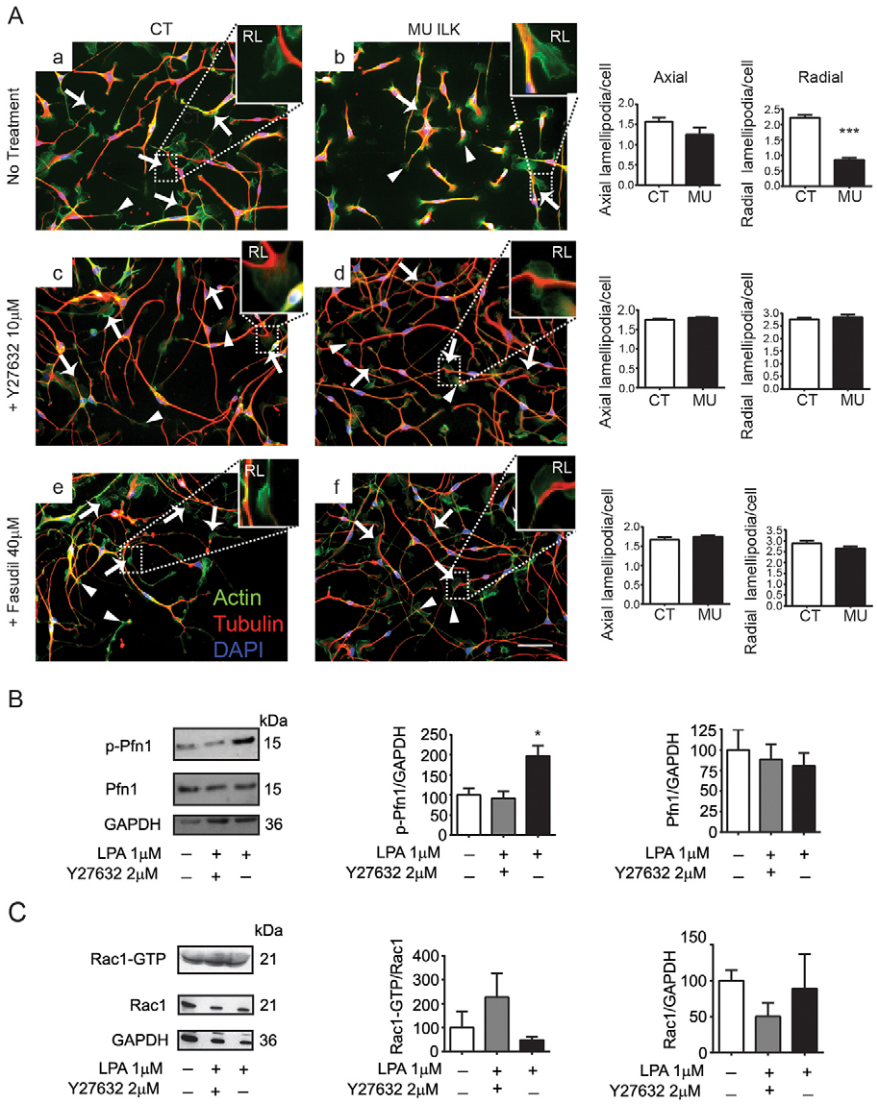

Fig. 1. Rho/ROCK regulates radial lamellipodia formation and Pfn1 phosphorylation in SCs. (A) Immunocytochemistry reveals the cytoskeleton of *Ilk* control and mutant SCs (a and b, c and d, e and f). Lamellipodia formed along SC processes (radial lamellipodia, arrows and magnified panels) or formed at the tip of the processes (axial lamellipodia, arrowheads) are depicted. *Ilk* mutant SCs form significant fewer radial lamellipodia (arrows) compared with controls (P=0.0003). No significant differences were seen in axial lamellipodia (arrowheads) (P=0.1955) (a,b), or in axial or radial lamellipodia between mutants and controls treated with ROCK inhibitor Y27632 (10 μM) (c,d) (P=0.1313 and P=0.5392, respectively) or fasudil (40 μM) (e,f) (P=0.3654 and P=0.2302, respectively). n=3 independent cell culture experiments. (B) Increased Pfn1 phosphorylation on Ser-137 in rat SCs treated with LPA (1 μM; 3 hours) (P=0.0192) compared with non-treated controls or SCs treated for 3 hours with Y27632 (2 μM) and LPA (1 μM). Total levels of Pfn1 were not significantly changed (P=0.7964). n=3 independent cell culture experiments. (C) Rac1 activity is not significantly changed in LPA-treated SCs (P=0.5288) compared with non-treated controls or SCs treated with Y27632 (2 μM) and LPA. Rac1 total levels are not significantly changed. n=3 independent cell culture experiments. Error bars indicate ±s.e.m. *P<0.05; ***P<0.001. Scale bar: 50 μm.

Development (2014) doi:10.1242/dev.101840

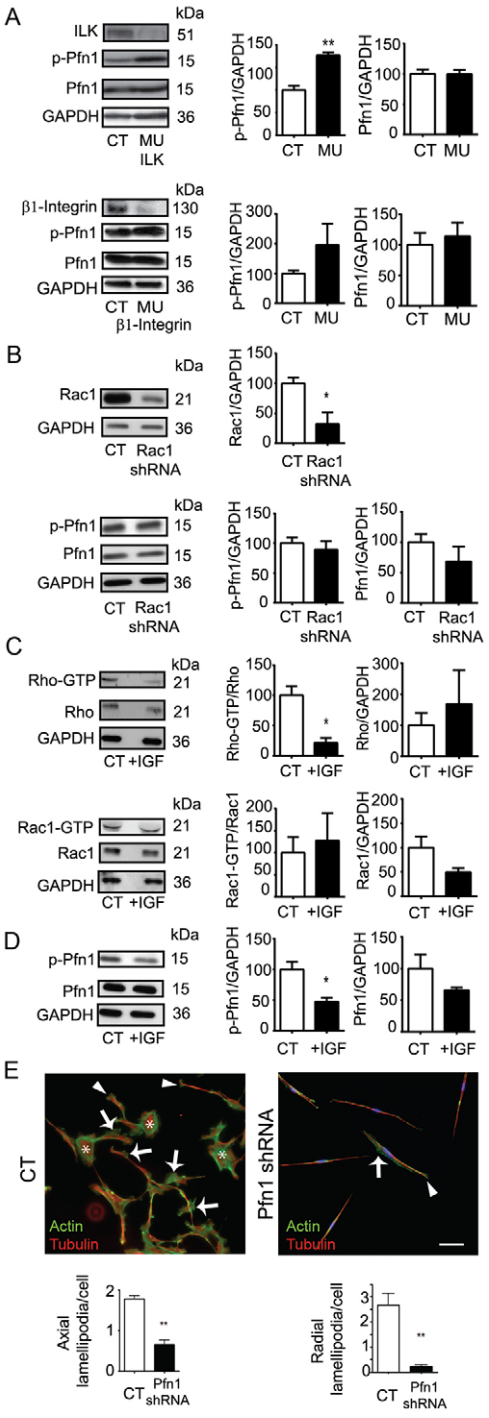

Fig. 2. The Rho/ROCK axis regulates Pfn1 phosphorylation, which affects lamellipodia formation. (A) Increased phospho-Pfn1 in protein lysates from P5 sciatic nerves of *Ilk* mutant mice (n=3 CT and MU mice, P=0.0024) compared with those of controls. Total levels of Pfn1 are not significantly changed (n=3 CT and MU mice, P=0.9750). Phospho-Pfn1 (n=3 CT and MU mice, P=0.2546) and Pfn1 total levels (n=3 CT and MU mice, P=0.6600) are not significantly changed in lysates from integrin β1 mutant SNs compared with those from controls. (B) Lentivirus-mediated knock-down of Rac1 in rat SCs significantly reduces Rac1 total levels (n=3 independent cell culture experiments; P=0.0345) compared with controls, but not Pfn1 phosphorylation (n=3 independent cell culture experiments; P=0.5574) or Pfn1 total levels (n=3 independent cell culture experiments; P=0.3169). (C) Igf1 treatment (150 ng/ml) decreases activation of RhoA, RhoB and RhoC (termed Rho) (n=3 independent cell culture experiments; P=0.0106), whereas their total levels (n=3 independent cell culture experiments; P=0.1075), the levels of activated Rac1 (n=3 independent cell culture experiments; P=0.7227) and Rac1 total levels (n=3 independent cell culture experiments; P=0.1075) are not significantly changed. The Rho antibody used is not specific for individual isoforms. (D) Pfn1 phosphorylation is significantly reduced in Igf1-treated SCs (n=3 independent cell culture experiments; P=0.0209) but not its total levels (n=3 independent cell culture experiments; P=0.2016). (E) Immunocytochemistry reveals the cytoskeleton of SCs infected with control or Pfn1-shRNA lentivirus. Pfn1-shRNA infection significantly decreases radial (arrows) (n=3 independent cell culture experiments; P=0.006) and axial (arrowheads) (n=3 independent cell culture experiments; P=0.0013) lamellipodia. Fibroblasts, when present, were excluded from the quantification (asterisks). Error bars indicate ±s.e.m. *P<0.05; **P<0.005. Scale bar: 50 μm.

western blotting showed some variability in the levels of both total and active Rac1 (Fig. 1C), such levels in untreated SCs and the levels in those SCs also treated with the ROCK inhibitor Y27632 or LPA were not significantly altered (Fig. 1C).

We hypothesized that Ilk-mediated negative regulation of Rho/ROCK signaling (Pereira et al., 2009) could promote SC lamellipodia formation via Pfn1 activation. Thus, we analyzed the levels of phospho-Pfn1 and total Pfn1 in lysates obtained from P5 and P14 *Ilk* mutant and control sciatic nerves (SNs) by western blot. We found that the levels of phospho-Pfn1 in mutant lysates were higher than those in controls and total levels of Pfn1 were unchanged (Fig. 2A, supplementary material Fig. S1).

Rac1 activity was not significantly altered by LPA treatment (Fig. 1C), and we had previously reported that high endogenous activation of Rac1 (Pereira et al., 2009) in *Ilk* mutant sciatic nerves did not counteract Rho/ROCK inhibition of lamellipodia formation. Thus, we postulated that Rho/ROCK and Rac1 could be working through independent downstream targets towards cytoskeleton remodeling and lamellipodia formation. To test this, we first analyzed phospho-Pfn1 and total Pfn1 levels in lysates obtained from P5 control and integrin β1 mutant sciatic nerves, in which Rac1 activation is decreased (Benninger et al., 2007; Nodari et al., 2007). We found that the levels of phospho-Pfn1 and total Pfn1 were not significantly changed in protein lysates from mutants (Fig. 2A). Then, to further confirm that Pfn1 phosphorylation is not Rac1 dependent, we knocked down Rac1 in SC cultures by lentiviral shRNA-mediated gene silencing (Fig. 2B) and analyzed the levels of phospho-Pfn1 and total Pfn1. We found no significant changes of either in lysates obtained from SC cultures after Rac1 knock down (Fig. 2B). Collectively, these results indicated that Rho/ROCK regulation of Pfn1 phosphorylation and function is indeed independent of Rac1 activation.

Igf1 modulates Rho/ROCK regulation of Pfn1

Igf1 is produced by SCs and promotes SC cytoskeleton remodeling (Cheng et al., 2000) and myelination (Ogata et al., 2006; Liang et al., 2007). Igf1 treatment of SCs resulted in a reduction in the levels of activated Rho and of phospho-Pfn1 compared with controls (Fig. 2C,D). Rac1 activity and total Rho, Rac1 and Pfn1 protein levels were not significantly changed (Fig. 2C,D). These data suggest that SC physiological stimuli, such as Igf1, can regulate lamellipodia formation by modulating ROCK/Pfn1 phosphorylation and, as a consequence, Pfn1 activity.

Pfn1 is required for SC lamellipodia formation, radial sorting and myelination

Lentiviral-mediated shRNA knockdown of Pfn1 in SCs reduced the formation of axial and radial lamellipodia compared with controls

Development (2014) doi:10.1242/dev.101840

(Fig. 2E). To examine its functions *in vivo*, we conditionally ablated *Pfn1* in SCs by expressing Cre recombinase under the control of the desert hedgehog (*Dhh*) gene regulatory sequences (Fig. 3A) (Jaegle et al., 2003). Although recombination of the conditional *Pfn1* allele (Fig. 3B) reduced Pfn1 protein levels in lysates obtained from P1 mutant SNs (Fig. 3C), Pfn2 levels remained unchanged (Fig. 3C). *In vitro*, *Pfn1* knockout SCs displayed reduced numbers of axial and radial lamellipodia, and these also appeared to be smaller and to contain less filamentous polymerized actin (Fig. 3D). *Pfn1* mutant mice were born at a sub-Mendelian frequency (<10%), and died of unknown causes at around P15. As a result, experiments were performed at P14 or earlier. P14 mutant sciatic nerves were thinner than those of controls (Fig. 3E). During postnatal development, immature SCs progressively segregate axons with a diameter over 1 µm. After having established a 1:1 relationship with such axons, pro-myelinating SCs will then myelinate them. This initial process, referred to as radial sorting, is usually complete by P14. Accordingly, at P0, SCs were present between bundles of tightly apposed axons in the sciatic nerves of control mice (Fig. 4Aa) and at P5 only few bundles still contained large caliber unsorted axons (Fig. 4Ac). Most of the large caliber axons were engaged in a 1:1 relationship with SCs (Fig. 4Ac). By P14, in control nerves all large caliber axons were sorted and myelinated (Fig. 4Ae). Only small caliber axons (less than 1 µm diameter) remained in so-called Remak bundles, surrounded by non-myelinating SCs. By contrast, in mutant sciatic nerves radial sorting and myelination were impaired. Bundles containing unsorted large caliber axons were still present in P14 mutant nerves (Fig. 4Af,C). More promyelinating SCs, meaning SCs in a 1:1 relationship with an axon without having produced myelin (Fig. 4Af,D), were also present. In addition, myelinated fibers that did form in mutants were thinner than those in control sciatic nerves (Fig. 4Ad,f, yellow arrowheads). Overall, the differentiation of SCs was severely impaired in the mutants. This conclusion was also supported by the findings that in P2 mutant sciatic nerves Oct6 expression was increased and Krox20 expression was reduced (Fig. 3F), compared with controls. The expression of Oct6 peaks at promyelinating and early myelinating stage, and is downregulated at later stages of myelination (Jaegle et al., 1996). Krox20 expression is required for downregulation of Oct6 and for the activation of myelin genes (Topilko et al., 1994). An insufficient number of SCs could also explain the persistence of axon bundles (Benninger et al., 2007; Grove et al., 2007). However, despite a slight increase in the percentage of apoptotic cells at P0 and P5 in mutant nerves (Fig. 3G), the number of proliferating Ki67-positive cells at different stages of development (Fig. 3G) and the total number of cells at P5 (Fig. 3G) were not significantly different from those in nerves from control mice.

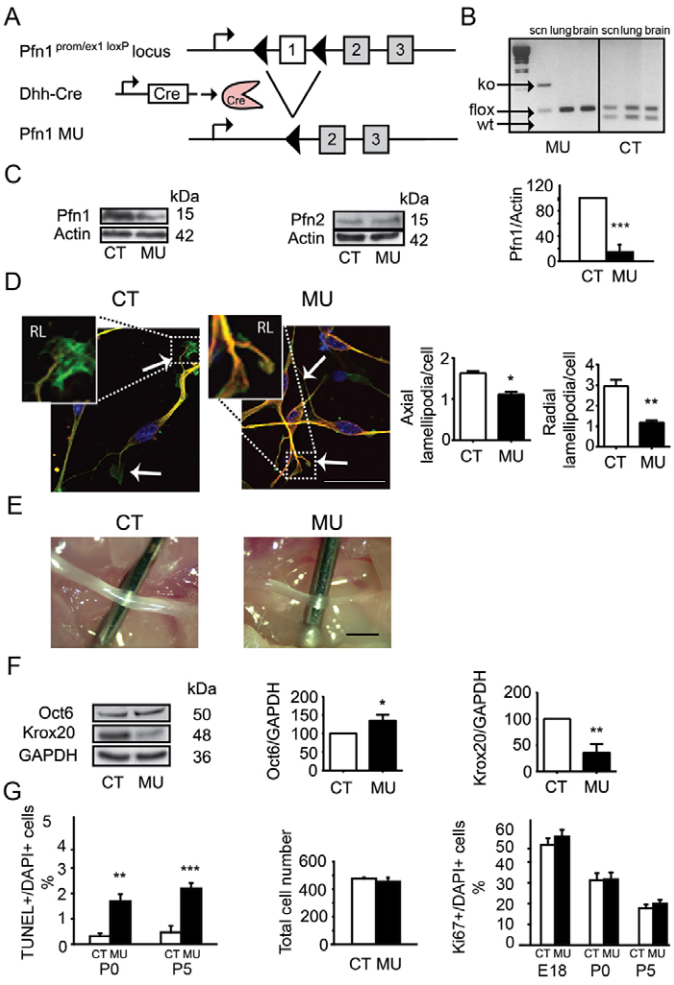

Fig. 3. Analysis of SC-specific Pfn1 mutant. (A) Upon *Dhh*-driven Cre recombination, the conditional *Pfn1* allele is inactivated. (B) PCR shows the recombination of the conditional *Pfn1* allele in genomic DNA isolated from P1 sciatic nerve, lung and brain of control and mutant mice. The fragment sizes for wild-type (wt), *Pfn1* floxed (flox) and *Pfn1* mutant (KO) alleles are indicated by black arrows. (C) Western blot analysis of protein lysates from P2 control and mutant SNs reveals that Pfn1 levels are reduced compared with controls (n=3 CT and MU mice; P=0.0001). Pfn2 expression was not significantly changed. (D) Immunocytochemistry reveals the cytoskeleton of *Pfn1* mutant and control SCs. *Pfn1* mutant SCs form reduced numbers of radial (n=3 independent cell culture experiments, P=0.0074) (arrows) and axial (n=3 independent cell culture experiments, P=0.0108) lamellipodia compared with controls. Scale bar: 50 µm. (E) SNs from P14 mutants are thinner and more transparent than those of control littermates. Scale bar: 1 mm. (F) Western blot analysis of protein lysates from P2 control and mutant SNs reveals that Oct6 levels are increased compared with controls (n=3 CT and MU mice, P=0.0216) and those of Krox20 are reduced (n=3 CT and MU mice, P=0.0024). (G) *Pfn1* mutant nerves contain significantly more TUNEL-positive, apoptotic cells at P0 (n=3 CT and MU sciatic nerves from 3 CT and MU mice, P=0.0011) and P5 (n=3 CT and MU sciatic nerves from 3 CT and MU mice, P=0.0006). However, the total number of cells in P5 control and mutant nerves was not changed. The numbers of Ki67-positive proliferating cells in E18, P0 and P5 control and mutant nerves were not significantly changed. Error bars indicate ±s.e.m. *P<0.05; **P<0.005; ***P<0.001.

To better understand why SC differentiation was impaired, we carried out a more detailed EM analysis of P5 and P14 control and mutant sciatic nerves (Fig. 4B). At P5, control SCs were at different stages of differentiation: immature SCs associated with axon bundles, promyelinating SCs in one-to-one relationship with axons, and a few myelinating SCs. In *Pfn1* mutant sciatic nerves, cytoplasmic processes of immature SCs enveloped the majority of axon bundles (Fig. 4Ba), and targeted and sorted axons (Fig. 4Ba). At the promyelination stage, SC-axon profiles in control and mutant nerves were surrounded by an apposed basal lamina (Fig. 4Bb,c,e, black arrows). In P14 control SNs, radial sorting of large caliber fibers was virtually complete. Mature SCs formed a compact multilayered sheath of myelin around single large caliber axons. In P14 mutant nerves, hypomyelination was pronounced (Fig. 4Ad,f,Bd, yellow arrowheads) and axon bundles enveloped by immature SCs still persisted. However, immature SCs were capable of enveloping axon bundles and only rarely were small sections of the axon bundle left naked (Fig. 4Bc, black arrowhead). The distinctive feature of these mutant nerves was the high number of SC-axon promyelinating profiles that did not progress to the mature

Development (2014) doi:10.1242/dev.101840

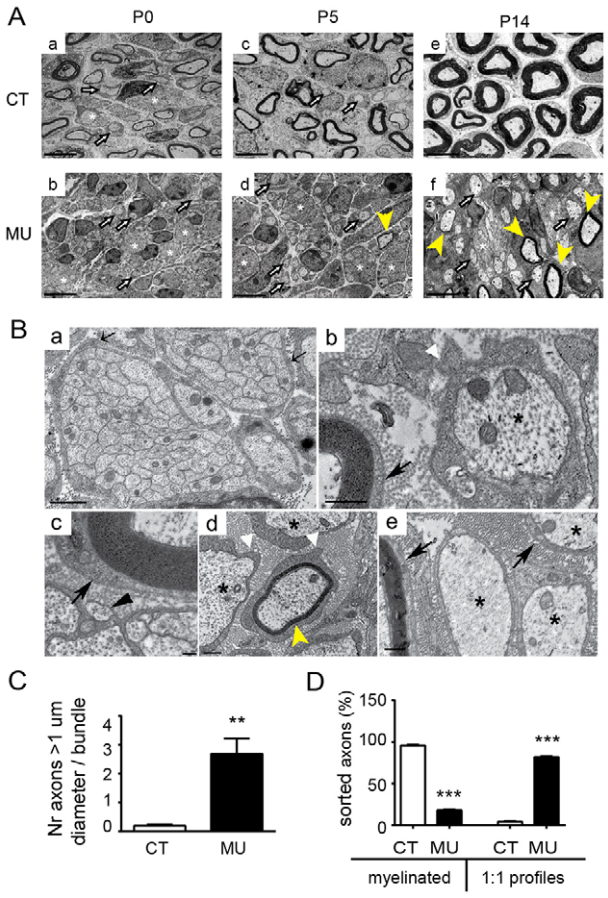

Fig. 4. Axonal sorting and myelination is impaired in *Dhh-Cre* Pfn1$^{l/l}$ mutant nerves. (A) Low-magnification EM micrographs of P0, P5 and P14 mutant and control sciatic nerve cross-sections (a-f). Whereas in control nerves individual axons are progressively sorted and myelinated (a, c and e), in mutant nerves bundles of unsorted axons (asterisks) and a large number of unmyelinated sorted axons (arrows) are present until P14 (f). Several axons show hypomyelination (yellow arrowheads). Scale bars: 4 µm. (B) High-magnification EM micrographs of mutant SN ultrathin sections. At P5, the majority of axon bundles are completely enveloped by immature SC processes (a, black arrows), and only rarely are a few naked areas visible (c, black arrowhead). SC-axon profiles are surrounded by basal lamina (black arrows) (b, c and e). Many P5 (b) and P14 (d,e) promyelinating SC-axon profiles (asterisks) are irregular in shape (white arrowheads). Scale bars: (a) 1 µm; (b) 0.5 µm; (c) 0.2 µm; (d) 0.5 µm; (e) 0.5 µm. (C) Bar graph showing quantification of the number of unsorted axons (with a diameter over 1 µm) per bundle in sciatic nerves (n=3 CT and MU mice, P=0.0037). P14 mutant sciatic nerves show a significant increase in the number of unsorted large caliber axons per bundle. (D) Bar graph showing the percentage of myelinated axons and the percentage of sorted axons blocked in a 1-to-1 relationship with SCs without being myelinated (1:1 profiles) in control and mutant sciatic nerves (n=3 CT and MU mice, P=0.0001). The percentage of 1:1 profiles is significantly higher in P14 mutant nerves than in controls. Error bars indicate ±s.e.m. **P<0.005; ***P<0.001.

myelinated form (Fig. 4Bb,d,e, asterisks). Mutant promyelinating SC-axon profiles were often irregular in shape and displayed abnormal cytoplasmic protrusions (Fig. 4Bb,d, white arrowheads). The Pfn1 mutant phenotype seemed to resemble that of the SC-specific *N-Wasp* (*Wasl* – Mouse Genome Informatics) mutant mouse (Jin et al., 2011; Novak et al., 2011), in which the diminished capacity of SCs to form lamellipodia at later stages affected mainly the ability to enwrap axons. This differed from the integrin β1 (Feltri et al., 2002), *Rac1* (Benninger et al., 2007; Nodari et al., 2007) or *Ilk* (Pereira et al., 2009) SC-conditional mutant mice, in which defects in radial lamellipodia formation affected mainly the capacity of SCs to sort axons, resulting in persistent sorting defects. In an attempt to study the effects of the loss of Pfn1 beyond P14, we conditionally ablated *Pfn1* by expressing Cre recombinase under the control of the 2′,3′-cyclic nucleotide 3′-phosphodiesterase (CNP) gene regulatory sequences (Lappe-Siefke et al., 2003). The SC phenotype of *CNP-Cre Pfn1*$^{fl/fl}$ mutant mice (Fig. 5), which were also born at a sub-Mendelian frequency, was similar to and at least as severe as that observed in the *Dhh-Cre* mutant mice. Nevertheless, a few *CNP-Cre Pfn1*$^{fl/fl}$ mutant mice survived beyond 3 weeks. The analysis of their phenotype at P24 was consistent with Pfn1 being required for efficient radial sorting and for promyelinating SCs to myelinate axons (Fig. 5). Similarly, in *Dhh-Cre Pfn1*$^{fl/fl}$ mutants, the nerves of P24 *CNP-Cre Pfn1*$^{fl/fl}$ mutant mice contained a large number of SC-axon promyelinating profiles that did not progress to myelination (Fig. 5Af,h, arrows; 5Be,f, #). The few of those that myelinated had thinner myelin sheaths (Fig. 5Ad,f,Be, yellow arrowheads), resulting in reduced fiber diameter versus axon diameter ratio in mutant sciatic nerves at P24 compared with controls (Fig. 5Ag). The myelin in mutant nerves was also significantly thinner compared with that of controls (Fig. 5H). Occasionally, some axon/SC profiles contained empty loops of redundant basal lamina (Fig. 5Bc, white arrows), interpreted before (Benninger et al., 2007; Pereira et al., 2009) as a sign of SC process instability.

DISCUSSION

Radial sorting and axon ensheathment by SCs are key events in the development of the PNS. They depend on laminin/integrin β1 interactions (Feltri et al., 2002), downstream activation of the small RhoGTPase Rac1 (Benninger et al., 2007; Nodari et al., 2007) via lymphoid cell kinase phosphorylation (Ness et al., 2013), and regulation of its targets N-WASP (Jin et al., 2011; Novak et al., 2011) and MLCK/myosin II (Wang et al., 2008; Leitman et al., 2011). Together with the negative regulation of Rho/ROCK signaling by Ilk (Pereira et al., 2009), they control SC cytoskeleton reorganization and the formation of SC lamellipodia largely through not yet fully characterized downstream targets and functional mechanisms.

In this study, using SC-specific gene ablation and other appropriate methodologies, we identify Pfn1, a G-actin-binding protein and ROCK substrate, as a novel key regulator of SCs lamellipodia formation, radial sorting and, of major impact, axon ensheathment during PNS development.

Pfn1 regulates SC radial lamellipodia independently of Rac1

Rac1 activity can directly regulate the number, extension and localization of lamellipodia in several cell types (Pankov et al., 2005). Although low levels of active Rac1 stimulate migratory behavior by inducing the formation of axial lamellipodia at the front and rear of fibroblasts and epithelial cells, higher levels of Rac1 stimulate cell adhesion and spreading by inducing the formation of radial lamellipodia around the whole perimeter of the cell (Pankov et al., 2005). Accordingly, Rac1 is essential for the formation of lamellipodia in SCs (Nodari et al., 2007). Its activation is mediated by ECM/integrin β1 interactions, mainly through LCK (Ness et al., 2013). Impairment of such interactions in SCs resulted in diminished Rac1 activation (Nodari et al., 2007) and consequently reduced radial lamellipodia formation and radial sorting (Feltri et al., 2002; Nodari et al., 2007). Positive modulation of lamellipodia formation by Rac1 is likely to be mediated, at least partially, through regulation of N-Wasp (Tomasevic et al., 2007; Jin et al., 2011; Novak et al., 2011).

Development (2014) doi:10.1242/dev.101840

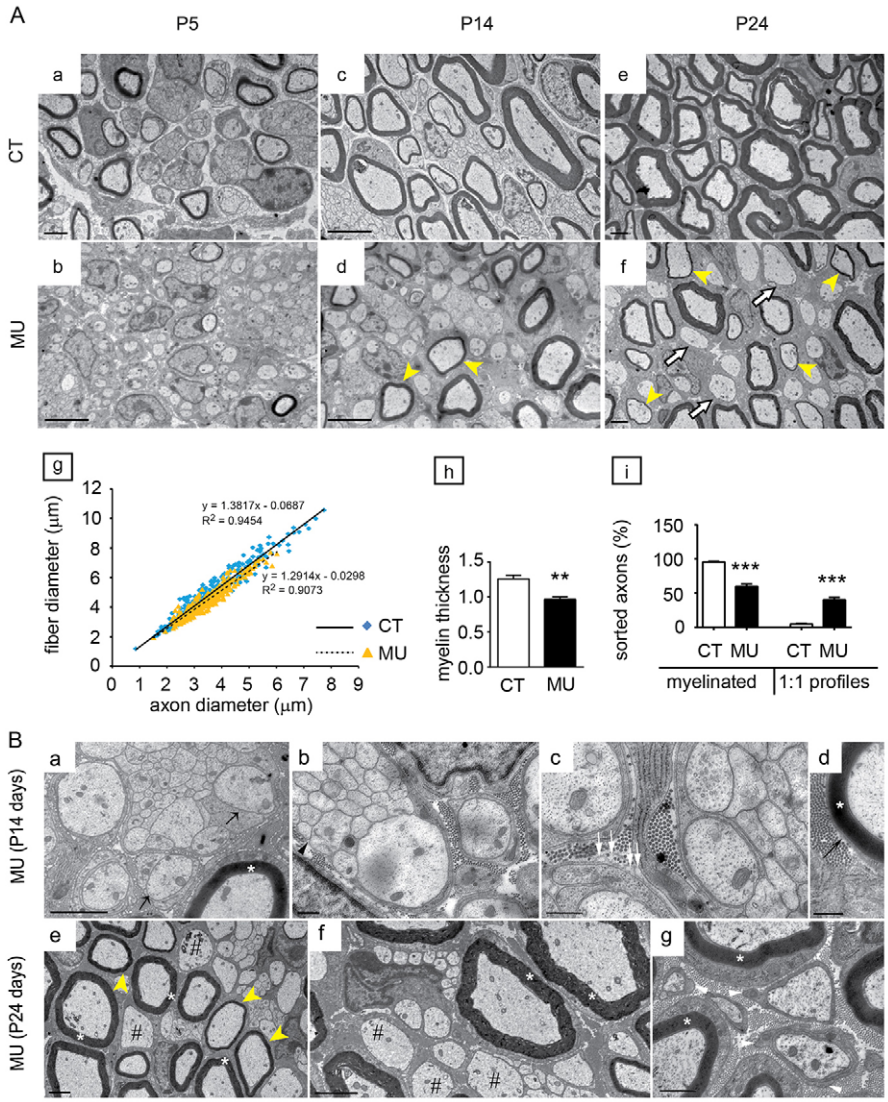

Fig. 5. Axonal sorting and myelination is impaired in *CNP-Cre* Pfn1$^{fl/fl}$ mutant nerves. (A) EM micrographs of P5, P14 and P24 control and mutant sciatic nerve cross-sections (a-f). Control axons are progressively sorted and myelinated (a, c and e). In mutant nerves, large numbers of promyelinating SC-axon profiles persist at P24 (arrows in f, and i). The ratio of fiber diameter versus axon diameter (g ratio) in mutant nerves is lower than in controls (g, 3 CT and MU mice). Quantitative analysis revealed that MU myelinated axons show significantly thinner myelin (d and f, yellow arrowheads; h, bar graph, *n*=3 CT and MU mice). Scale bars: 2 μm in a, e, f; 5 μm in b-d. (B) High-magnification EM micrographs of P14 and P24 mutant SN show a phenotype similar to that described for *Dhh-Cre Pfn1* mutants (Fig. 4). Immature SC processes (black arrows in a) envelop axon bundles, and only occasionally are a few naked areas visible (b, black arrowheads). Myelinated SC-axon profiles are surrounded by basal lamina (black arrow in d). Large numbers of promyelinating SC-axon profiles persist at P24 (e and f, #), and many are irregular in shape, displaying abnormal cytoplasmic protrusions (white arrowheads in g) at the cell surface. Occasionally, redundant basal lamina loops are present (white arrows, c). Some myelinating SC-axon profiles are present (a, d, e, f and g, white asterisks) and are hypomyelinated (e, yellow arrowheads). Scale bars: 2 μm in a,f; 0.5 μm in b,d; 1 μm in c; 5 μm in e; 1 μm in g.

Radial sorting was also defective in SC-specific Ilk mutant mice (Pereira et al., 2009). Ilk is a negative regulator of Rho/ROCK signaling, and injections of the ROCK inhibitor fasudil in *Ilk* mutant mice were able to re-establish radial sorting to control levels (Pereira et al., 2009). In line with this, we show that Ilk-deficient SCs form fewer radial lamellipodia compared with controls, and that pharmacological inhibition of ROCK by Y27632 or fasudil is sufficient to restore lamellipodia formation. In *Ilk* mutant sciatic nerves, Rac1 activity is significantly increased in relation to controls (Pereira et al., 2009). As this is not sufficient to counteract Rho/ROCK activation and to prevent radial sorting and axon ensheathing defects, we hypothesized that Rho/ROCK and Rac1 signaling might act on independent downstream targets in promoting lamellipodia formation, radial sorting and axon ensheathment.

Pfn1 is a ROCK substrate (Shao et al., 2008) known to promote lamellipodia formation in different cell types (Cao et al., 1992; Syriani et al., 2008). Accordingly, we show that in SCs exposed to LPA or in *Ilk* mutant sciatic nerves in which ROCK activation is increased, Pfn1 is phosphorylated on Ser-137 by ROCK.

Under our experimental conditions, Pfn1 phosphorylation seems not to be dependent on Rac1 activation, as knocking down Rac1 in SCs had no effect on the levels of Pfn1 phosphorylation. Although we cannot exclude that very short LPA exposure could transiently induce Rac1 activation in primary SCs [similarly to what was reported by Barber and colleagues (Barber et al., 2004) for the SCL4.1/F7 SC line], it is unlikely that such an early and short activation could overcome the long lasting Rho/ROCK activation and resulting Pfn1 phosphorylation observed in this study. Such conclusion is also supported by the fact that the Rac1 hyperactivation seen in *Ilk* mutant mice could not counteract the defects on SC lamellipodia formation, radial sorting and myelination present on those mice (Pereira et al., 2009). Overall, our data suggest that Pfn1 is a Rho/ROCK-specific downstream target in the regulation of SC lamellipodia formation. In point of fact, exposure of SCs to Igf1, which is known to promote SC lamellipodia formation (Cheng et al., 2000), can reduce the activation levels of Rho and phospho-Pfn1 without significantly changing Rac1 activation. Using lentiviral-mediated shRNA gene silencing, and conditional gene ablation in SCs, we demonstrate that Pfn1 is indeed essential for SC radial lamellipodia formation.

Pfn1 regulates radial sorting and axon ensheathment

SC-specific *Pfn1* gene ablation profoundly impaired radial sorting and axon ensheathment in sciatic nerves of mutant mice. Although we also observed a strong delay in radial sorting, the main feature of both *Dhh-Cre* and *CNP-Cre Pfn1$^{f/f}$* mutant SNs was the presence

Development (2014) doi:10.1242/dev.101840

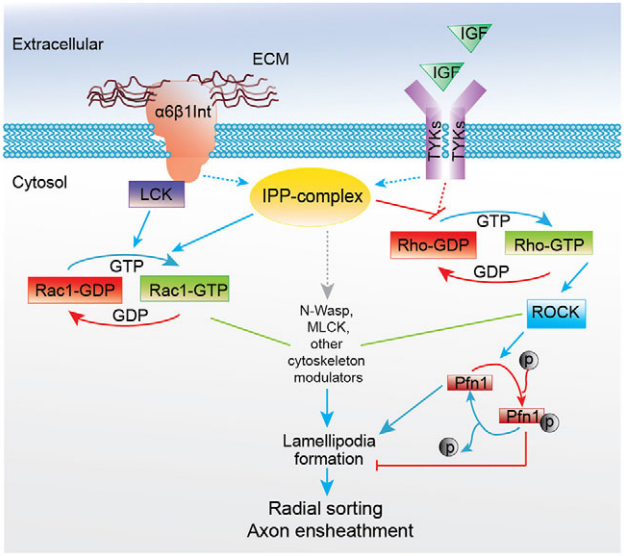

Fig. 6. Integrated scheme of functional signaling mechanisms mediating radial lamellipodia formation and myelination downstream of the IPP complex and of β1 integrin. Igf1 and/or the IPP-complex (Pereira et al., 2009) negatively regulate Rho/ROCK activation. This translates into the modulation of downstream effectors that are crucial for SC myelination. Thus, decreased phosphorylation of the ROCK substrate Pfn1 mediates SC lamellipodia formation, promoting radial sorting and ensheathment. These processes are co-regulated by integrin β1 (Feltri et al., 2002), which activates (blue line) Rac1 (Benninger et al., 2007; Nodari et al., 2007) mainly via laminin/integrin-β1/lymphoid cell kinase (LCK) tyrosine kinase (Ness et al., 2013) also modulating the activity of cytoskeletal remodeling proteins, e.g. MLCK/myosin II (Wang et al., 2008; Leitman et al., 2011) and N-Wasp (Jin et al., 2011; Novak et al., 2011). These are crucial in mediating lamellipodia formation and SC myelination. Rho/ROCK-mediated Pfn1 phosphorylation is sufficient to counteract Rac1 activation, causing the failure of SCs radial lamellipodia formation, radial sorting and axon ensheathment. Inhibition is indicated by a red line; activation is indicated by blue line; modulation is indicated by a green line. ECM, extracellular matrix; IPP, Ilk-Pinch-Parvin; TYKs, tyrosine receptor kinases.

of a large number of promyelinating SC-axon profiles that persisted at P24, the latest time point analyzed (Fig. 5). This delay in radial sorting and the deficits in axon ensheathment were likely to be caused by increased F-actin instability at the lamellipodia (Birbach, 2008).

In neurons and in other cell types, Pfn is thought to participate in the reorganization of the actin cytoskeleton by binding to actin and to a plethora of cytoskeleton-regulating proteins with proline-rich domains, such as Ena/Mena/VASP family members, and N-WASP, which, as mentioned above, has recently been implicated in radial sorting (Jin et al., 2011; Novak et al., 2011). Pfn can also directly bind to membrane phospholipids, mainly PtdIns(4,5)P_2 [phosphatidylinositol (4,5)-bisphosphate] and PtdIns(3,4,5)P_3 (Lassing and Lindberg, 1985), linking lipid-based signaling pathways to the actin cytoskeleton (Birbach, 2008). Local availability of Pfn helps to stabilize lamellipodia and other actin-based structures. Its absence causes local instability of the actin cytoskeleton, which in *Drosophila* leads to premature arrest of axons during pathfinding (Wills et al., 1999). Consistent with a role for Pfn in controlling actin stability, promyelinating SC-axon profiles in mutants were often irregular in shape and displayed abnormal cytoplasmic protrusions, occasionally containing empty loops of redundant basal lamina, a likely sign of SC process instability (Benninger et al., 2007; Pereira et al., 2009).

It is thought that a minimum threshold number of SCs is required to initiate radial sorting (Martin and Webster, 1973; Webster, 1971). Ablation of genes involved in SC proliferation, such as *Cdc42* (Benninger et al., 2007) or *Fak* (Grove et al., 2007) results in radial sorting impairment. In *Pfn1*-mutant nerves, SC proliferation was not affected, and despite a slight increase in SC death the total number of SCs was normal. Therefore, similar to integrin β1 (Feltri et al., 2002), *Rac1* (Benninger et al., 2007; Nodari et al., 2007) and *Ilk* (Pereira et al., 2009) mutant nerves, we consider it likely that the radial sorting and axon ensheathment defects observed are a direct consequence of deficits in radial lamellipodia formation.

The complex nature of radial sorting and axon ensheathment is likely to depend on the strict control exerted by multiple crosstalking signaling pathways, including those modulating Ilk/Rho/ROCK or integrin β1/LCK/Rac1 activation (Fig. 6). Such pathways control several cytoskeleton modulators, including N-WASP (Tomasevic et al., 2007; Jin et al., 2011; Novak et al., 2011) and MLCK/myosin II (Wang et al., 2008; Leitman et al., 2011), that are key in regulating radial lamellipodia formation, an essential requirement for radial sorting and axon ensheathing. Although Rac1 is a positive regulator, promoting radial lamellipodia and radial sorting, Rho/ROCK can counteract it as a negative regulator, repressing their formation. Our data show for the first time that the G-actin binding protein Pfn1, a ROCK substrate, is essential for SC radial lamellipodia formation and consequently for radial sorting and axon ensheathing. The fact that somehow unexpectedly one single ROCK effector can have such a profound impact on SC development and myelination justifies the need for a better characterization of other molecular players participating in these and other related pathways. This knowledge is crucial for a better understanding of PNS development in health and disease.

MATERIALS AND METHODS

Animals

All animal experiments were performed with the approval and in strict accordance with the guidelines of the Swiss Cantonal Veterinary Office, the Portuguese Veterinary Office and EU directives. All efforts were made to minimize animal suffering, reduce the number of required animals and replace with *in vitro* experiments whenever possible.

Generation of conditional knockout mice

Mice homozygous for the integrin-β1 floxed allele were crossed with mice expressing Cre recombinase under the control of the 2′,3′-cyclic nucleotide 3′-phosphodiesterase (*CNPase*) promoter (‘knock-in’) (Lappe-Siefke et al., 2003; Saher et al., 2005; Grove et al., 2007) and which were heterozygous for the floxed allele, as previously described (Benninger et al., 2006; Thurnherr et al., 2006). Mice homozygous for the *Rac1* or the *Ilk* floxed allele were crossed with mice expressing Cre recombinase under the control of the desert hedgehog (*Dhh*) promoter (Jaegle et al., 2003) and which were heterozygous for the floxed allele, as previously described (Benninger et al., 2007; Pereira et al., 2009).

Mice homozygous for the *Pfn1* floxed allele were crossed with mice expressing the Cre recombinase under the control of either the *Dhh* or *CNPase* promoter and heterozygous for the *Pfn1* floxed allele (Böttcher et al., 2009). Progeny of interest were *Cre*+ *Pfn1*$^{lox/lox}$ mice (hereafter called mutant mice), and *Cre*+ *Pfn1*$^{lox/wt}$ (hereafter called control mice). All genotypes were determined by PCR on genomic DNA. All experiments were performed on mice kept on a C57Bl/6 background.

Antibodies

Mouse anti-Gapdh (WB 1:10,000, Hytest), rabbit anti-alpha-tubulin (ICC 1:2000, Abcam, UK), Rat anti-Ki67 (ICC 1:50, DAKO, Denmark), rabbit anti-Oct6 (WB 1:1000), rabbit anti-Krox20 (WB 1:100, BabCO), mouse anti-Rho (WB 1:2000, Upstate), rabbit anti-Ilk (WB 1:1000, Abcam, UK),

rabbit anti-β1-integrin (WB 1:500, Abcam, UK), mouse and rabbit anti-Pfn1 (WB 1:1000, Abcam, UK), rabbit anti-Pfn2 (WB 1:500, kindly provided by Prof. R. Fässler, Martinsried, Germany), rabbit anti-phosphoSer137 Pfn1 (WB 1:1000, kindly provided by Dr Marc Diamond, UCSF, San Francisco, USA), mouse anti-Rac1 (WB 1:1000, BD Biosciences, USA), goat anti-mouse IgG HRP coupled (WB 1:15,000, Jackson Laboratories, PA, USA), donkey anti-rabbit IgG HRP coupled (WB 1:10,000, Jackson Laboratories, PA, USA), goat anti-rat IgG HRP coupled (WB 1:10,000, Jackson Laboratories, PA, US), goat anti-mouse IgG H-L Cy3 coupled (ICC 1:3000, Jackson Laboratories, PA, USA).

Electron microscopy

Mice were anesthetized and perfused with 0.1 M phosphate buffer (pH 7.4), followed by 3% glutaraldehyde and 4% paraformaldehyde. Fixed tissues were dehydrated through a graded acetone series, post-fixed in 2% osmium-tetroxide, and embedded in 'Spurr's resin' (Electron Microscopy Sciences). Semi-thin sections were stained with 1% Toluidine Blue for light microscopy, and ultrathin sections on grids with 3% uranyl acetate, 1% lead citrate, before examination in a Hitachi H-600 and a Jeol 1400 transmission electron microscope.

Primary Schwann cell culture

Mouse SC cultures were obtained from P0-P2 sciatic nerves. Nerves were digested [0.7 mg/ml collagenase type I, 0.25% trypsin (Invitrogen) in Hank's balanced salt solution (Invitrogen)]. After trituration, cells were grown on poly-D-lysine/laminin 2-coated dishes in minimal medium plus 0.5% FBS. Minimal medium is DMEM+Glutamax (Gibco), human apo-transferrin (100 µg/ml), progesterone (60 ng/ml), insulin (5 µg/ml), putrescine (16 µg/ml), L-thyroxin (400 ng/ml), selenium (160 ng/ml), triiodothyronine (10 ng/ml) and BSA (300 µg/ml, Fluka). Rat SC cultures were obtained from P2-P3 Wistar rats sciatic nerves. Nerves were digested in 1% collagenase in HBSS (Invitrogen). Cells were grown on poly-D-lysine/laminin 2-coated dishes in DMEM+Glutamax (GIBCO), 10% FBS (GIBCO), 1% penicillin/streptomycin, Forskolin (2 µM) and neuregulin 1 (5 ng/ml), following fibroblasts complement-mediated cytolysis with anti-Thy1.1 antibody. Supplements were from Sigma unless stated otherwise.

Lysophosphatidic acid (LPA)/ROCK and Igf1 activation assay

LPA assay was performed as previously described (Weiner et al., 2001). Rat SCs were serum starved overnight (16-18 hours) in modified SATO medium (DMEM+Glutamax, 1× N2 supplement, 20 µg/ml pituitary extract, 0.1 mg/ml BSA, 4 µM forskolin and penicillin/streptomycin). Cells were treated with 1 µM LPA for 3 hours. ROCK activation was blocked by pretreatment with Y27632 (2 µM) for 10 minutes. For Igf1 activation assay, cells were serum starved and treated for 1 hour with 150 ng/ml recombinant Igf1 (Invitrogen).

For SC cultures, three independent experiments were performed (minimum number of counted cells per experimental condition for each *n*: Ilk CT/MU SCs=minimum 60 cells per condition per *n*; all others=minimum 25 cells per condition per *n*).

Rho-GTPase activity

The glutathione S-transferase-p21-activated kinase-Cdc42/Rac interactive binding motif domain (GST-PAK-CD) construct was kindly provided by J. Collard (The Netherlands Cancer Institute, Amsterdam). GST-tagged rhotekin Rho-binding domain protein was purchased from Millipore. Rac1 and pan-Rho activity were measured as described previously (Benninger et al., 2007; Pereira et al., 2009). In brief, cells were homogenized in FISH buffer (10% glycerol, 50 mM Tris-HCl (pH 7.4), 100 mM NaCl, 1% NP-40, 2 mM $MgCl_2$ and protease inhibitor cocktail (Sigma-Aldrich) and centrifuged for 5 minutes at 13,000 ***g*** at 4°C. Aliquots of exactly 10% of the volume were taken to determine the total protein amounts. The remaining supernatant was incubated with the bait proteins bound to glutathione-coupled Sepharose beads (GE Healthcare) at 4°C for 30 minutes. Beads and proteins bound to the fusion protein were washed three times in excess of FISH buffer, eluted in Laemmli sample buffer and analyzed for bound Rac1 or pan-Rho by immunoblotting.

Immunofluorescence and TUNEL assay

For immunohistochemistry, sciatic nerve sections were blocked for 1 hour with 10% goat serum, 0.1% Triton X-100, in PBS and incubated with primary antibodies overnight (4°C). Tissue sections were washed (1× PBS) and incubated with secondary antibodies (1 hour, room temperature). Sections were mounted in Citifluor (Citifluor) containing 4′,6′-diamidino-2-phenylindole (DAPI).

For immunocytochemistry cultures were fixed in 4% PFA in MP buffer [65 mM PIPES, 25 mM HEPES, 10 mM EGTA, 3 mM $MgCl_2$ (pH 6.9)] for 10 minutes at room temperature. After permeabilization (0.1% Triton X-100, PBS) for 5 minutes at room temperature, cells were incubated with primary monoclonal antibodies (2% goat serum, PBS) 1 hour at room temperature, followed by secondary conjugated antibodies and DAPI. Coverslips were mounted on Superfrost glass-slides with Shandon ImmuMount (Thermo Scientific). F-actin was stained with the toxin Phalloidin-Alexa488 (ICC 1:50, Molecular Probes, Invitrogen, Carlsbad, USA).

Apoptotic cell death was analyzed by TUNEL staining using biotin-labeled-UTP and FITC-conjugated-streptavidin according to the manufacturer's instructions (Roche Diagnostics). Images were acquired using a Zeiss fluorescence microscope with Zeiss Axiocam CCD camera and AxioVisionV4.5 (Zeiss) acquisition software. Images were processed using Adobe Photoshop V8.0.

Immunoblotting

Tissues and cells were homogenized in RIPA lysis buffer [0.1% SDS, 10 mM Tris-HCl, 150 mM NaCl, 50 mM NaF, 1 mM $NaVO_4$, 1 mM EDTA, 0.5% sodium-deoxycholate, protease inhibitor cocktail (Sigma)]. Extracts were processed using standard SDS-PAGE and immunoblotting procedures. X-ray films were scanned on a GS-800 calibrated densitometer (Bio-Rad), using Quantity One software (Bio-Rad). Only images containing bands with no saturated pixels, confirmed by the software detection system color coding saturated pixels in red, were used for subsequent quantification. Densitometry and quantification of the relative levels were carried out with ImageJ software.

Statistical analysis

Data show mean±s.e.m. Statistical significance was determined using a two-tailed Student's *t*-test, when two groups were compared, or one-/two-way analysis of variance when multiple groups were compared. Significance was set at $*P<0.05$, $**P<0.01$, $***P<0.001$.

Acknowledgements

We thank M. Diamond for the phospho-Pfn1 antibody and Ned Mantei for critically reading the manuscript. This work is dedicated to the memory of our friend and colleague Yves Benninger.

Competing interests

The authors declare no competing financial interests.

Author contributions

L.M., T.B.-T., U.S. and J.B.R. were responsible for the project and experimental design. L.M., T.B.-T., J.P.F., J.A.P., N.G.D., R.F., A.B., Y.B., A.F.G., R.T.B., M.C., K.-A.N., R.J.M.F. and D.M. were responsible for experimental work/data analysis. L.M., T.B.-T., J.A.P., U.S. and J.B.R. wrote and edited the manuscript and prepared the figures.

Funding

Work in the J.B.R. lab was funded by the European Regional Development Fund (FEDER), Operational Competitiveness Programme COMPETE, by the Foundation for Science and Technology (FCT) [FCOMP-01-0124-FEDER-007048 (PTDC/BIA-BCM/69841/2006) and FCOMP-01-0124-FEDER-014190 (PTDC/BIA-BCM/112730/2009)] and by the International Foundation for Research in Paraplegia, Zurich. Work in U.S.'s lab was funded by the Swiss National Science Foundation (SNSF) and by the National Center of Competence in Research Neural Plasticity and Repair. L.M. was supported by a Marie-Curie fellowship [AXOGLIA, 236766] and by a Swiss National Science Foundation Marie Heim-Voegtlin fellowship. J.P.F. and A.F.G. were supported by an FCT fellowship [BPD/SFRH/34834/2007, 28640/2006].

Supplementary material

Supplementary material available online at
http://dev.biologists.org/lookup/suppl/doi:10.1242/dev.101840/-/DC1

References

Barber, S. C., Mellor, H., Gampel, A. and Scolding, N. J. (2004). S1P and LPA trigger Schwann cell actin changes and migration. *Eur. J. Neurosci.* **19**, 3142-3150.

Benninger, Y., Colognato, H., Thurnherr, T., Franklin, R. J., Leone, D. P., Atanasoski, S., Nave, K. A., Ffrench-Constant, C., Suter, U. and Relvas, J. B. (2006). Beta1-integrin signaling mediates premyelinating oligodendrocyte survival but is not required for CNS myelination and remyelination. *J. Neurosci.* **26**, 7665-7673.

Benninger, Y., Thurnherr, T., Pereira, J. A., Krause, S., Wu, X., Chrostek-Grashoff, A., Herzog, D., Nave, K. A., Franklin, R. J., Meijer, D. et al. (2007). Essential and distinct roles for cdc42 and rac1 in the regulation of Schwann cell biology during peripheral nervous system development. *J. Cell Biol.* **177**, 1051-1061.

Birbach, A. (2008) Profilin, a multi-modal regulator of neuronal plasticity. *BioEssays* **30**, 994-1002.

Böttcher, R. T., Wiesner, S., Braun, A., Wimmer, R., Berna, A., Elad, N., Medalia, O., Pfeifer, A., Aszódi, A., Costell, M. et al. (2009). Profilin 1 is required for abscission during late cytokinesis of chondrocytes. *EMBO J.* **28**, 1157-1169.

Cao, L. G., Babcock, G. G., Rubenstein, P. A. and Wang, Y. L. (1992). Effects of profilin and profilactin on actin structure and function in living cells. *J. Cell Biol.* **117**, 1023-1029.

Carlsson, L., Nyström, L. E., Sundkvist, I., Markey, F. and Lindberg, U. (1977). Actin polymerizability is influenced by profilin, a low molecular weight protein in non-muscle cells. *J. Mol. Biol.* **115**, 465-483.

Cheng, H. L., Steinway, M. L., Russell, J. W. and Feldman, E. L. (2000). GTPases and phosphatidylinositol 3-kinase are critical for insulin-like growth factor-I-mediated Schwann cell motility. *J. Biol. Chem.* **275**, 27197-27204.

Da Silva, J. S., Medina, M., Zuliani, C., Di Nardo, A., Witke, W. and Dotti, C. G. (2003). RhoA/ROCK regulation of neuritogenesis via profilin IIa-mediated control of actin stability. *J. Cell Biol.* **162**, 1267-1279.

Feltri, M. L., Graus Porta, D., Previtali, S. C., Nodari, A., Migliavacca, B., Cassetti, A., Littlewood-Evans, A., Reichardt, L. F., Messing, A., Quattrini, A. et al. (2002). Conditional disruption of beta 1 integrin in Schwann cells impedes interactions with axons. *J. Cell Biol.* **156**, 199-210.

Feltri, M. L., Suter, U. and Relvas, J. B. (2008). The function of RhoGTPases in axon ensheathment and myelination. *Glia* **56**, 1508-1517.

Finkel, T., Theriot, J. A., Dise, K. R., Tomaselli, G. F. and Goldschmidt-Clermont, P. J. (1994). Dynamic actin structures stabilized by profilin. *Proc. Natl. Acad. Sci. USA* **91**, 1510-1514.

Grove, M., Komiyama, N. H., Nave, K. A., Grant, S. G., Sherman, D. L. and Brophy, P. J. (2007). FAK is required for axonal sorting by Schwann cells. *J. Cell Biol.* **176**, 277-282.

Jaegle, M., Mandemakers, W., Broos, L., Zwart, R., Karis, A., Visser, P., Grosveld, F. and Meijer, D. (1996). The POU factor Oct-6 and Schwann cell differentiation. *Science* **273**, 507-510.

Jaegle, M., Ghazvini, M., Mandemakers, W., Piirsoo, M., Driegen, S., Levavasseur, F., Raghoenath, S., Grosveld, F. and Meijer, D. (2003). The POU proteins Brn-2 and Oct-6 share important functions in Schwann cell development. *Genes Dev.* **17**, 1380-1391.

Jessen, K. R. and Mirsky, R. (2005). The origin and development of glial cells in peripheral nerves. *Nat. Rev. Neurosci.* **6**, 671-682.

Jin, F., Dong, B., Georgiou, J., Jiang, Q., Zhang, J., Bharioke, A., Qiu, F., Lommel, S., Feltri, M. L., Wrabetz, L. et al. (2011). N-WASp is required for Schwann cell cytoskeletal dynamics, normal myelin gene expression and peripheral nerve myelination. *Development* **138**, 1329-1337.

Lambrechts, A., Braun, A., Jonckheere, V., Aszodi, A., Lanier, L. M., Robbens, J., Van Colen, I., Vandekerckhove, J., Fässler, R. and Ampe, C. (2000). Profilin II is alternatively spliced, resulting in profilin isoforms that are differentially expressed and have distinct biochemical properties. *Mol. Cell. Biol.* **20**, 8209-8219.

Lappe-Siefke, C., Goebbels, S., Gravel, M., Nicksch, E., Lee, J., Braun, P. E., Griffiths, I. R. and Nave, K. A. (2003). Disruption of Cnp1 uncouples oligodendroglial functions in axonal support and myelination. *Nat. Genet.* **33**, 366-374.

Lassing, I. and Lindberg, U. (1985). Specific interaction between phosphatidylinositol 4,5-bisphosphate and profilactin. *Nature* **314**, 472-474.

Leitman, E. M., Tewari, A., Horn, M., Urbanski, M., Damanakis, E., Einheber, S., Salzer, J. L., de Lanerolle, P. and Melendez-Vasquez, C. V. (2011). MLCK regulates Schwann cell cytoskeletal organization, differentiation and myelination. *J. Cell Sci.* **124**, 3784-3796.

Liang, G., Cline, G. W. and Macica, C. M. (2007). IGF-1 stimulates de novo fatty acid biosynthesis by Schwann cells during myelination. *Glia* **55**, 632-641.

Martin, J. R. and Webster, H. D. (1973). Mitotic Schwann cells in developing nerve: their changes in shape, fine structure, and axon relationships. *Dev. Biol.* **32**, 417-431

Ness, J. K., Snyder, K. M. and Tapinos, N. (2013). Lck tyrosine kinase mediates β1-integrin signalling to regulate Schwann cell migration and myelination. *Nat. Commun.* **4**, 1912.

Nodari, A., Zambroni, D., Quattrini, A., Court, F. A., D'Urso, A., Recchia, A., Tybulewicz, V. L., Wrabetz, L. and Feltri, M. L. (2007). Beta1 integrin activates Rac1 in Schwann cells to generate radial lamellae during axonal sorting and myelination. *J. Cell Biol.* **177**, 1063-1075.

Novak, N., Bar, V., Sabanay, H., Frechter, S., Jaegle, M., Snapper, S. B., Meijer, D. and Peles, E. (2011). N-WASP is required for membrane wrapping and myelination by Schwann cells. *J. Cell Biol.* **192**, 243-250.

Ogata, T., Yamamoto, S., Nakamura, K. and Tanaka, S. (2006). Signaling axis in schwann cell proliferation and differentiation. *Mol. Neurobiol.* **33**, 51-62.

Pankov, R., Endo, Y., Even-Ram, S., Araki, M., Clark, K., Cukierman, E., Matsumoto, K. and Yamada, K. M. (2005). A Rac switch regulates random versus directionally persistent cell migration. *J. Cell Biol.* **170**, 793-802.

Pereira, J. A., Benninger, Y., Baumann, R., Gonçalves, A. F., Ozçelik, M., Thurnherr, T., Tricaud, N., Meijer, D., Fässler, R., Suter, U. et al. (2009). Integrin-linked kinase is required for radial sorting of axons and Schwann cell remyelination in the peripheral nervous system. *J. Cell Biol.* **185**, 147-161.

Saher, G., Brügger, B., Lappe-Siefke, C., Möbius, W., Tozawa, R., Wehr, M. C., Wieland, F., Ishibashi, S. and Nave, K. A. (2005). High cholesterol level is essential for myelin membrane growth. *Nat. Neurosci.* **8**, 468-475.

Shao, J., Welch, W. J., Diprospero, N. A. and Diamond, M. I. (2008). Phosphorylation of profilin by ROCK1 regulates polyglutamine aggregation. *Mol. Cell. Biol.* **28**, 5196-5208.

Syriani, E., Gomez-Cabrero, A., Bosch, M., Moya, A., Abad, E., Gual, A., Gasull, X. and Morales, M. (2008). Profilin induces lamellipodia by growth factor-independent mechanism. *FASEB J.* **22**, 1581-1596.

Thurnherr, T., Benninger, Y., Wu, X., Chrostek, A., Krause, S. M., Nave, K. A., Franklin, R. J., Brakebusch, C., Suter, U. and Relvas, J. B. (2006). Cdc42 and Rac1 signaling are both required for and act synergistically in the correct formation of myelin sheaths in the CNS. *J. Neurosci.* **26**, 10110-10119.

Tomasevic, N., Jia, Z., Russel, A., Fujii, T., Hartman, J. J., Clancy, S., Wang, M., Beraud, C., Wood, K. W. and Sakowicz, R. (2007). Differential regulation of WASP and N-WASP by Cdc42, Rac1, Nck, and PI(4,5)P2. *Biochemistry* **46**, 3494-3502.

Topilko, P., Schneider-Maunoury, S., Levi, G., Baron-Van Evercooren, A., Chennoufi, A. B., Seitanidou, T., Babinet, C. and Charnay, P. (1994). Krox-20 controls myelination in the peripheral nervous system. *Nature* **371**, 796-799.

Wang, H., Tewari, A., Einheber, S., Salzer, J. L. and Melendez-Vasquez, C. V. (2008). Myosin II has distinct functions in PNS and CNS myelin sheath formation. *J. Cell Biol.* **182**, 1171-1184.

Webster, H. D. (1971) Myelinogenesis. Structural aspects. *Neurosci. Rel. Program Bull.* **9**, 470-477.

Webster, H. D., Martin, R. and O'Connell, M. F. (1973). The relationships between interphase Schwann cells and axons before myelination: a quantitative electron microscopic study. *Dev. Biol.* **32**, 401-416.

Weiner, J. A., Fukushima, N., Contos, J. J., Scherer, S. S. and Chun, J. (2001). Regulation of Schwann cell morphology and adhesion by receptor-mediated lysophosphatidic acid signaling. *J. Neurosci.* **21**, 7069-7078.

Wills, Z., Marr, L., Zinn, K., Goodman, C. S. and Van Vactor, D. (1999). Profilin and the Abl tyrosine kinase are required for motor axon outgrowth in the Drosophila embryo. *Neuron* **22**, 291-299.

Witke, W. (2004). The role of profilin complexes in cell motility and other cellular processes. *Trends Cell Biol.* **14**, 461-469.

Witke, W., Podtelejnikov, A. V., Di Nardo, A., Sutherland, J. D., Gurniak, C. B., Dotti, C. and Mann, M. (1998). In mouse brain profilin I and profilin II associate with regulators of the endocytic pathway and actin assembly. *EMBO J.* **17**, 967-976.

Witke, W., Sutherland, J. D., Sharpe, A., Arai, M. and Kwiatkowski, D. J. (2001). Profilin I is essential for cell survival and cell division in early mouse development. *Proc. Natl. Acad. Sci. USA* **98**, 3832-3836.

Wu, C. H., Fallini, C., Ticozzi, N., Keagle, P. J., Sapp, P. C., Piotrowska, K., Lowe, P., Koppers, M., McKenna-Yasek, D., Baron, D. M. et al. (2012). Mutations in the profilin 1 gene cause familial amyotrophic lateral sclerosis. *Nature* **488**, 499-503.

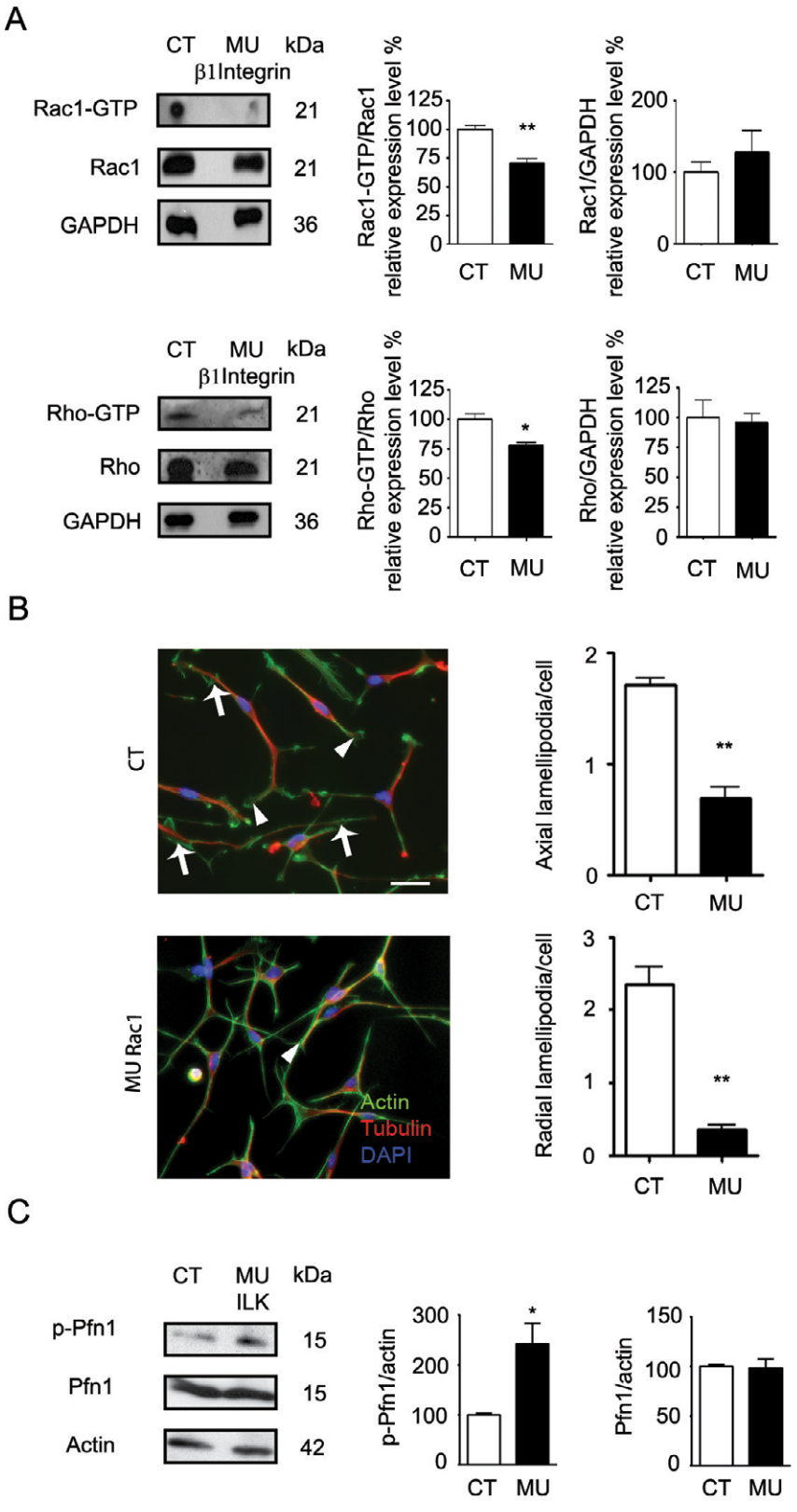

Fig. S1. Integrin-β1/rac1 promotes SC lamellipodia formation. (A) Reduced rac1 activation (*n*=3, *P*=0.003) and rho activation (*n*=3, *P*=0.0103) in protein lysates obtained from P5 integrin-β1 mutant sciatic nerves. Total rac1 (*n*=3, *P*=0.4445) and total rho (*n*=3, *P*=0.7767) were not significantly changed. (B) Immunocytochemistry reveals the cytoskeleton of rac1 mutant and control SCs. The number of radial (arrows) (*n*=3, *P*=0.0013) and axial lamellipodia (arrow heads) (*n*=3, *P*=0.0012) is significantly reduced compared to controls. Error bars indicate±s.e.m. **P*<0.05; ***P*<0.005. Bar, 20 µm. (C) Increased phospho-Pfn1 in protein lysates from P14 sciatic nerves of *Ilk* mutant mice (*n*=3 CT and MU mice, *P*=0.028) compared with those of controls (*n*=3 CT and MU mice, *P*=0.028). Total levels of Pfn1 are not significantly changed (*n*=3 CT and MU mice, *P*=0.8736).